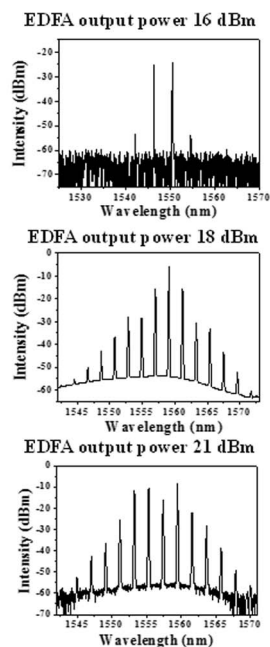
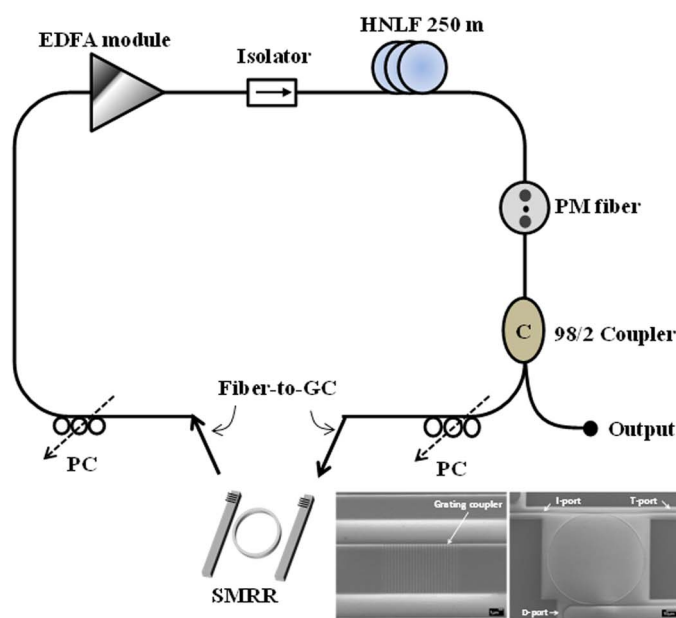


250-GHz Passive Harmonic Mode-Locked Er-Doped Fiber Laser by Dissipative Four-Wave Mixing With Silicon-Based Micro-Ring

Volume 5, Number 5, October 2013

Siao-Shan Jyu
 Ling-Gang Yang
 Chi-Yan Wong
 Chien-Hung Yeh, Member, IEEE
 Chi-Wai Chow, Senior Member, IEEE
 Hon-Ki Tsang, Senior Member, IEEE
 Yinchieh Lai



DOI: 10.1109/JPHOT.2013.2283243
 1943-0655 © 2013 IEEE

250-GHz Passive Harmonic Mode-Locked Er-Doped Fiber Laser by Dissipative Four-Wave Mixing With Silicon-Based Micro-Ring

Siao-Shan Jyu,¹ Ling-Gang Yang,¹ Chi-Yan Wong,²
Chien-Hung Yeh,^{3,4} *Member, IEEE*, Chi-Wai Chow,¹ *Senior Member, IEEE*,
Hon-Ki Tsang,² *Senior Member, IEEE*, and Yinchieh Lai¹

¹Department of Photonics and Institute of Electro-Optical Engineering, National Chiao Tung University, Hsinchu 30010, Taiwan

²Department of Electronic Engineering, The Chinese University of Hong Kong, Hong Kong

³Information and Communications Research Laboratories, Industrial Technology Research Institute (ITRI), Hsinchu 31040, Taiwan

⁴Graduate Institute of Applied Science and Engineering, Fu Jen Catholic University, New Taipei 24205, Taiwan

DOI: 10.1109/JPHOT.2013.2283243
1943-0655 © 2013 IEEE

Manuscript received August 14, 2013; revised September 13, 2013; accepted September 18, 2013. Date of current version October 2, 2013. This work was supported by the National Science Council Taiwan, under Contracts NSC-101-2622-E-009-009-CC2, NSC-101-2628-E-009-007-MY3, NSC-100-2221-E-009-088-MY3, and NSC-102-2221-E-009-152-MY3; by the Ministry of Education, Taiwan; and by the Hong Kong Research Grants Council under Grant GRF CUHK416710. Corresponding author: C.-W. Chow (e-mail: cwchow@faculty.nctu.edu.tw).

Abstract: We propose and demonstrate a 250-GHz high-repetition-rate mode-locked Er-doped fiber laser, which utilizes a silicon micro-ring resonator (SMRR). The SMRR acts as an optical comb filter to help achieve passive mode-locking through the dissipative four-wave-mixing effect induced by a piece of high nonlinear fiber. A short section of polarization-maintaining fiber is inserted in the cavity to induce birefringence filtering to significantly enhance the stability of the proposed laser through the combined effects of optical filtering and nonlinear spectral broadening. The laser can operate about 2 and 6 nm in the case of 1.48-ps and 875-fs output pulsewidth, with 3-dB bandwidth, respectively. The laser can remain mode locked, during our measurement time, without any cavity length or temperature feedback control.

Index Terms: Fiber lasers, optical communications, four-wave mixing (FWM).

1. Introduction

Ultra-fast pulse lasers have played important roles in many research areas, such as high speed optical communications [1]–[4]. In the literature, many techniques have been developed to increase the pulse repetition rate. The active rational harmonic mode-locking techniques can be implemented by detuning the electro-optic (EO) modulation frequency with a rational ratio of the cavity fundamental repetition frequency to achieve the pulse repetition rate multiplication [5], [6]. Besides, passive mode-locking techniques which utilize dissipative four-wave-mixing (DFWM) effects [7]–[10] along with optical comb filtering to produce mode-locked pulse trains with the repetition rate defined by the comb spacing have also been developed. Sub-THz repetition rates have been demonstrated successfully, and the intra-cavity optical comb filtering can be achieved by many

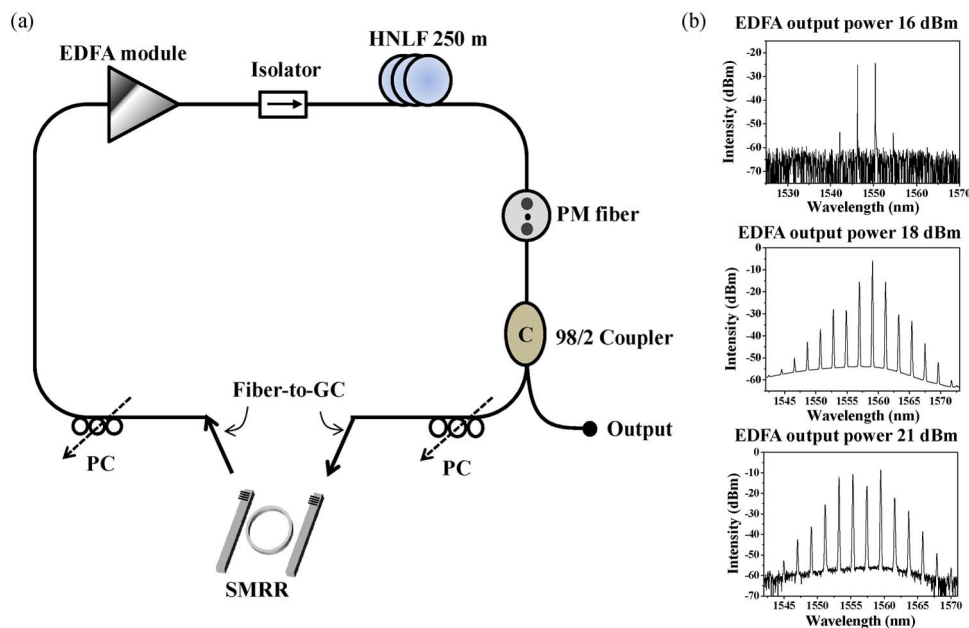


Fig. 1. (a) Schematic diagram of 250-GHz passive harmonic mode-locked Er-doped fiber laser with a silicon-based micro-ring resonator. (b) The optical spectra with different power levels from continuous-wave to mode-locked states.

means including a Fabry-Perot filter [8], a sampled fiber Bragg grating [9], a programmable optical processor [10], and a micro-ring resonator [11]. In ref. [11], the multi-bound pulse state can be observed in a mode-locked fiber laser based on a silicon micro-ring resonator (SMRR). In view of the recent development trends of silicon photonics [12], [13], it will be interesting to utilize SMRR for building high repetition rate mode-locked fiber lasers. The SMRR acts as an intra-cavity optical comb filter, and hence, the exact round-trip size is required. Mature CMOS fabrication affords precise size control of micro-ring [12].

In the present work, we propose and demonstrate a 250-GHz high-repetition-rate mode-locked Er-doped fiber laser which utilizes an SMRR for intra-cavity optical comb filtering, which has a free-spectral-range (FSR) of 2 nm. The SMRR acts as an optical comb filter to help achieve passive mode-locking through the dissipative four-wave mixing (FWM) effect induced by a piece of high nonlinear fiber (HNLf). A short section of polarization maintaining fiber (PMF) is inserted in the cavity to induce birefringence filtering to significantly enhance the stability of the proposed laser through the combined effects of optical filtering and nonlinear spectral broadening. The laser can operate in the case of 1.48 ps output pulse-width with 3-dB bandwidth about 2 nm and the case of 875 fs output pulse-width with 3-dB bandwidth about 6 nm. To the best of our knowledge, this is the first work which utilizes the silicon-based micro-ring for building mode-locked fiber laser operating up to the 250 GHz repetition rate. The laser can remain mode-locked during our measurement time (> 1 h) without any cavity length or temperature feedback control.

2. Experiment

The detailed experimental setup of our proposed laser is shown in Fig. 1(a). The laser system is composed of (i) one commercial C-band Er-fiber amplifier (EDFA) module as the gain medium (S-Series Booster EDFA at C-band by GIP Corporation, 21 dBm output saturation power); (ii) two manual polarization controllers (PCs) for intra-cavity polarization control; (iii) one silicon-on-insulator (SOI)-based SMRR with polarization dependent grating coupler (GC) as the optical comb filter and polarizer; (iv) one section of 250 m HNLf for enhancing the FWM effects (group velocity dispersion = 0.86 ps/nm/km, nonlinear coefficient = $10.7 \text{ W}^{-1}\text{km}^{-1}$). To couple the lights between the single mode fiber (SMF) and the SMRR effectively, the GC technique was used.

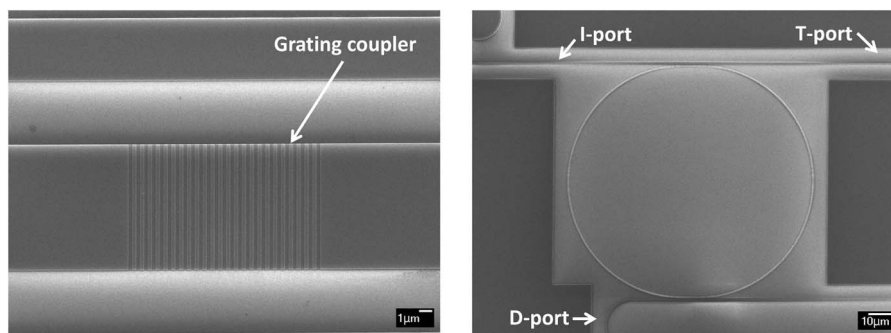


Fig. 2. SEM photography of (a) grating coupler with $14\ \mu\text{m}$ in length, $9\ \mu\text{m}$ in width, and $580\ \text{nm}$ in period; (b) silicon micro-ring resonator with two silicon nano-wires, the input port (I-port) and the drop port (D-port).

Inside the laser cavity, the polarization independent isolator enforces the optical pulses to propagate in single direction. The SMRR only allows the optical harmonic modes with $2\ \text{nm}$ spacing to build up by the filtering effect. The phases of these modes will be locked by the FWM effect induced by the HNLF. We have also inserted a short ($1\ \text{cm}$) section of PMF in the cavity, as shown in Fig. 1(a). The introduced birefringence by the PMF with the polarization dependence of the GCs of the SMRR can act as a Lyot filter to help stabilize the laser through the combined effects of optical filtering and nonlinear spectral broadening. We have found that this is a very crucial step for achieving stable laser operation. With all of these set up correctly, the laser can be mode-locked stably by adjusting the two PCs. Typical output optical spectra of the laser at different EDFA output power levels are shown in Fig. 1(b). When the EDFA output power is $16\ \text{dBm}$, the laser spectrum exhibits four optical modes. When the power level is increased to $18\ \text{dBm}$, ten optical modes build up. When the power is finally increased to $21\ \text{dBm}$, 12 optical modes with higher optical power are observed, as shown in Fig. 1(b).

The silicon-chip containing the SMRR and GCs was fabricated by using the deep-ultra-violet (DUV) 193-nm lithography and the reactive ion etching (RIE) techniques on a SOI wafer with a $0.22\ \mu\text{m}$ top silicon layer and a $2\ \mu\text{m}$ buried oxide (BOX) layer. The GCs are $14\ \mu\text{m}$ long and $9\ \mu\text{m}$ wide with $580\ \text{nm}$ in period and $70\ \text{nm}$ in depth. The SMRR is composed of two straight silicon waveguides and a ring waveguide. The straight waveguides are $500\ \text{nm}$ wide and $220\ \text{nm}$ high, which support only the fundamental mode. The total length of straight waveguides is less than $1\ \text{cm}$. For the ring structure, the length of the straight coupling region (CR) and the circumference of the ring are $6\ \mu\text{m}$ and $232\ \mu\text{m}$, respectively. The gap between the ring and the straight waveguide is $200\ \text{nm}$. The 3-dB filtering bandwidth is $0.04\ \text{nm}$ at the resonant wavelength of $1546\ \text{nm}$, and the Q value is 3.8×10^4 . The images of scanning-electron-microscopy (SEM) for the GCs and SMRR are shown in Fig. 2(a) and (b), respectively. The add-drop configuration of the SMRR is also shown in Fig. 2(b), where the I-port, T-port, and D-port denote the input-port, throughput-port, and drop-port, respectively. The SMRR operates as a narrow band-pass comb filter to allow the resonant wavelengths to pass from the I-port to D-port. The GCs are designed for coupling lights into the TE mode of the waveguide. The optimum incident angle from the fiber to the GC is with an off-vertical tilt angle of 10° , and the measured net coupling loss is $\sim 7\ \text{dB/grating}$. Within the off-set optical launching range of $-2.5 \sim 4\ \mu\text{m}$ in the x-z plane, the additional loss caused by the offset is less than $1\ \text{dB}$. Hence, very precise optical launching between the fiber and the SMRR is not required. The coupling efficiency can be further improved if apodized grating structure were used [14]. The SMRR acts as an intra-cavity optical comb filter, and hence, the exact round-trip size is required. Mature CMOS fabrication affords precise size control of micro-ring.

3. Results and Discussion

Figs. 3 and 4 show the experimental optical spectra and second-harmonic generation (SHG) auto-correlation traces of the proposed laser measured at the EDFA powers of $18\ \text{dBm}$ and $21\ \text{dBm}$,

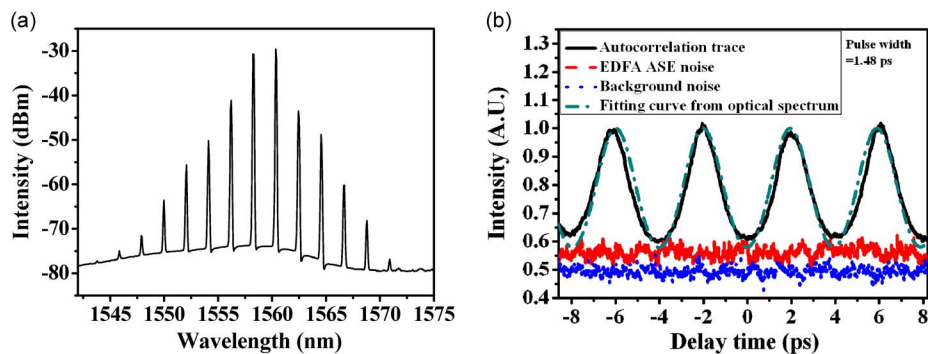


Fig. 3. (a) Measured optical spectrum of the laser output (bandwidth = 2 nm, 10 lasing modes above -70 dBm power level); (b) autocorrelation trace of the 250 GHz pulse train (pulse width = 1.48 ps, fitted with the measured spectral distribution from the optical spectrum).

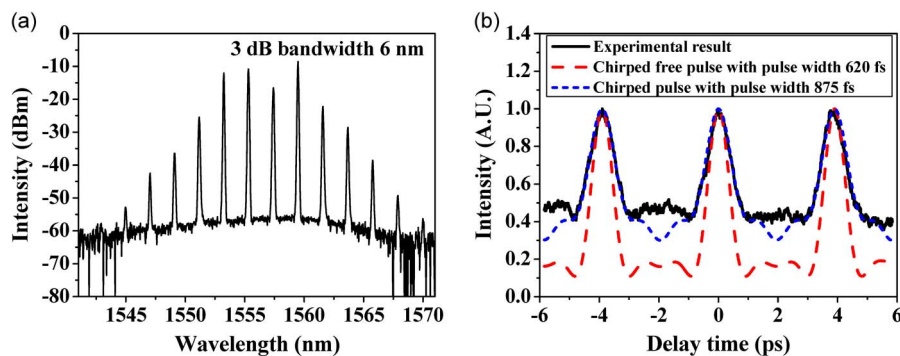


Fig. 4. (a) Optical spectrum of the laser output (bandwidth = 6 nm, 12 lasing modes above -65 dBm power level); (b) autocorrelation trace of the 250 GHz pulse train (pulse width = 875 fs, fitted with the measured spectral distribution from the optical spectrum).

respectively. The optical spectrum shown in Fig. 3(a) has ten optical modes above -70 dBm with 2 nm optical bandwidth. The noise background in the optical spectrum comes from the amplified spontaneous emission (ASE) noises of the booster EDFA. The laser output power from the 2% port is about 2 mW. An additional booster EDFA is used to amplify the pulse train before the autocorrelation measurement. In Fig. 3(b), the measured SHG intensity autocorrelation trace is plotted as the solid black line. The period of the pulse train is 4 ps, which corresponds to the 250 GHz repetition rate. The autocorrelation traces of the ASE without optical pulse train and the background noise are also shown in Fig. 3(b) for reference. The noise floor in the autocorrelation trace is mainly contributed by the background noise of the equipment. In order to determine the actual pulse-width from the autocorrelation trace data, the relative spectral distribution of the harmonic modes is directly estimated from the measured optical spectrum data. When the phases of all these modes are assumed to be the same and with the addition of the equipment measurement floor, we obtain the fitted dashed green line in Fig. 3(b) and a pulse-width of 1.48 ps can be obtained.

Fig. 4(a) shows that the measured optical spectrum for the proposed laser is operated at sub-picosecond case. The optical bandwidth is about 6 nm, and 12 harmonic modes above -65 dBm can be seen. When the phases of all these modes are assumed to be the same, one obtains the dashed red line in Fig. 4(b). It is obvious that the fitting width is smaller than the experimental data. To account for this, a suitable second order chirp is then added to best fit the autocorrelation trace, which is shown as the dotted blue line in the same figure. The time domain FMHM pulse-width is then determined to be about 875 fs from the fitting, and the time-bandwidth product is about 0.65. In principle, a suitable length of dispersion compensation fiber can be placed outside the laser cavity

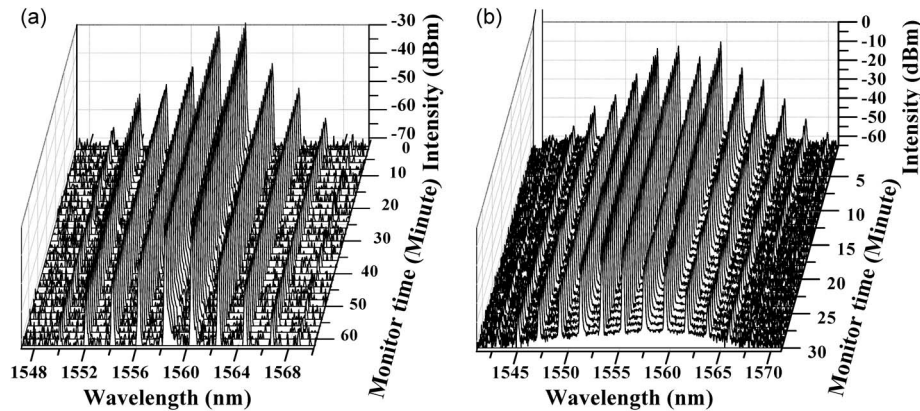


Fig. 5. Stability measurement of the optical spectra (a) of the 10 lasing modes case and (b) of the 12 lasing modes case.

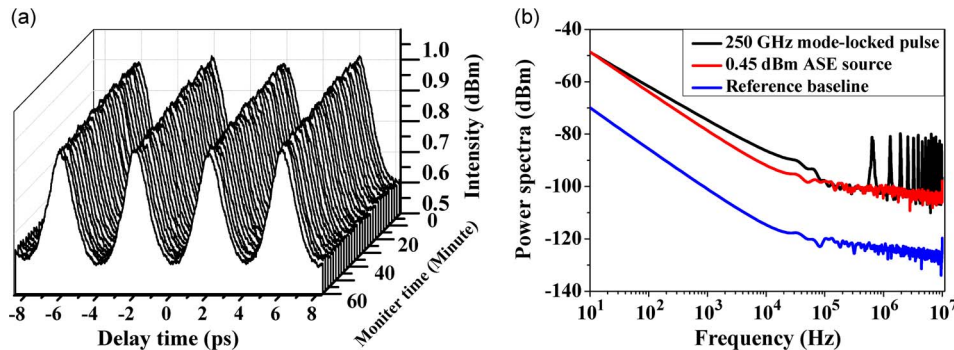


Fig. 6. (a) Stability measurement of autocorrelation trace within 60 minutes and (b) laser intensity noise spectrum (measurement resolution = 10 Hz).

to produce chirp-less pulses if the chirp is mainly linear. There are also some background contributions from the measurement floor of the auto-correlator in the measured trace data.

Experimentally, the laser can be self-started when the pumping power is high enough, and the PCs are set appropriately. To perform the mode-locking experiment, we simply adjust the PCs by monitoring the optical spectrum. The 250 GHz spacing mode-locking frequency components can be easily observed on an optical spectrum analyzer (OSA). This provides the required indication for optimally adjusting the PCs.

To monitor the stability of mode-locking operation, we use an OSA to record the output optical spectra in a period of time > 30 min. The results are shown in Fig. 5. We observe that the main mode-locked harmonic modes remain mode-locked stably with small frequency shift on the order of $0.01 \sim 0.02$ nm, which is close to the resolution limit of our OSA. The harmonic modes in both sides of the spectrum will slightly fluctuate since their energies are low.

To more definitely prove that the mode-locking can be maintained in a reasonably long period of time, the measured auto-correlation traces within one hour are plotted in Fig. 6(a) (the ten lasing mode case). The results demonstrate that the laser can remain mode-locked without any feedback control in a typical lab environment. The power spectra intensity of the laser is illustrated in Fig. 6(b). We inject the optical power of 0.45 dBm from the laser output port into a DC coupled photo-detector (EOTech ET-3010) and use an RF spectrum analyzer (Agilent E4440A) to measure the RF spectrum. The black line is the power spectrum intensity of the laser, the red line is that for 0.45 dBm ASE noises (for the comparison purpose), and the blue line is the reference baseline signal (without

any injected optical power) from the measurement system. No large oscillation frequencies are observed within the measurement range, except some small super-mode beating noises at the harmonic frequencies of the cavity modes. This also demonstrates that the laser should be reasonably well mode-locked. It is also worth to mention that similar results are obtained in the 12 lasing mode case. The laser can easily stay mode-locked longer than one hour without using any feedback control. Additional cavity length feedback control will be needed in order to maintain the mode-locking at a much longer period of time.

In principle, the lasing characteristics depend on several laser parameters. We use a PMF and PCs to form a Lyot-type filter, which induces birefringence filtering to significantly enhance the stability of the proposed laser through the combined effects of optical filtering and nonlinear spectral broadening. The adjustment of PCs is also crucial. Different setting of the PCs can make the laser to be mode-locked at different states (single-pulse and bound-pulse) or to become only CW lasing. Other laser parameters like the filter bandwidth of the micro-ring, the intra-cavity optical loss, and the length of the HNLFF may also have impacts on the laser performance and can be further optimized.

4. Conclusion

We proposed and demonstrated a 250 GHz high repetition rate mode-locked fiber laser operating in the C-band. The laser employed a silicon photonics SMRR with an FSR of 2 nm to act as an optical comb filter for achieving passive mode-locking at the 250 GHz rate through the dissipative FWM. A short section of PMF was inserted in the cavity to induce birefringence filtering to significantly enhance the stability of the proposed laser through the combined effects of optical filtering and nonlinear spectral broadening. The uniform tapered GC technique with an off-vertical coupling angle was used to insert the SMRR inside the fiber ring cavity with tolerable insertion loss. To the best of our knowledge, this is the first work which utilizes the silicon-based micro-ring for building mode-locked fiber lasers operating up to the 250 GHz repetition rate. This should open up many new possibilities to integrate mode-locked fiber lasers with silicon photonics. We characterized the optical spectra, SHG autocorrelation trace, and the power spectra intensity of the proposed laser. The laser can operate in the case of 1.48 ps output pulse-width with 3-dB bandwidth about 2 nm and the case of 875 fs output pulse-width with 3-dB bandwidth about 6 nm. The proposed laser can remain mode-locked during our measurement time (> 1 h) without any cavity length or temperature feedback control.

References

- [1] J.-W. Shi, J.-W. Lin, C.-B. Huang, F.-M. Kuo, N.-W. Chen, C.-L. Pan, and J. E. Bowers, "Photonic generation of few-cycle millimeter-wave pulse using a waveguide-based photonic-transmitter-mixer," *IEEE Photon. J.*, vol. 4, no. 4, pp. 1071–1079, Aug. 2012.
- [2] C. W. Chow, F. M. Kuo, J. W. Shi, C. H. Yeh, Y. F. Wu, C. H. Wang, Y. T. Li, and C. L. Pan, "100 GHz ultra-wideband (UWB) fiber-to-the-antenna (FTTA) system for in-building and in-home networks," *Opt. Exp.*, vol. 18, no. 2, pp. 473–478, Jan. 2010.
- [3] P. C. Peng, J. F. Chen, H. H. Lu, and Y. T. Lin, "Wavelength-tunable optical pulse generation from a fiber ring laser with a reflective semiconductor optical amplifier," *Laser Phys.*, vol. 21, no. 3, pp. 509–511, Mar. 2011.
- [4] J.-H. Lin and K.-H. Lin, "Multiple pulsing and harmonic mode-locking in an all-normal-dispersion Nd:GdVO₄ laser using a nonlinear mirror," *J. Phys. B, At. Mol. Opt. Phys.*, vol. 436, pp. 065402-1–065402-6, Mar. 2010.
- [5] C. Wu and N. K. Dutta, "High-repetition-rate optical pulse generation using a rational harmonic mode-locked fiber laser," *IEEE J. Quantum Electron.*, vol. 36, no. 2, pp. 145–150, Feb. 2000.
- [6] S.-S. Jyu, G.-H. Jiang, and Y. Lai, "Laser dynamics of asynchronous rational harmonic mode-locked fiber soliton lasers," *Laser Phys.*, vol. 23, no. 8, p. 085106, Jul. 2013.
- [7] M. Quiroga-Teixeiro, C. Balslev Clausen, M. P. Sorensen, P. L. Christiansen, and P. A. Andrekson, "Passive mode locking by dissipative four-wave mixing," *J. Opt. Soc. Amer. B, Opt. Phys.*, vol. 15, no. 4, pp. 1315–1321, Apr. 1998.
- [8] E. Yoshida and M. Nakazawa, "Low-threshold 115-GHz continuous-wave modulational-instability erbium-doped fiber laser," *Opt. Lett.*, vol. 22, no. 18, pp. 1409–1411, Sep. 1997.
- [9] S. Zhang, F. Lu, X. Dong, P. Shum, X. Yang, X. Zhou, Y. Gong, and C. Lu, "Passive mode locking at harmonics of the free spectral range of the intracavity filter in a fiber ring laser," *Opt. Lett.*, vol. 30, no. 21, pp. 2852–2854, Nov. 2005.

- [10] J. Schröder, T. D. Vo, and B. J. Eggleton, "Repetition-rate-selective, wavelength-tunable mode-locked laser at up to 640 GHz," *Opt. Lett.*, vol. 34, no. 24, pp. 3902–3904, Dec. 2009.
- [11] S.-S. Jyu, L.-G. Yang, C.-H. Yeh, C. W. Chow, H. K. Tsang, and Y. Lai, "Multi-bound pulse state in a 250 GHz mode-locked fiber laser based on a silicon micro-ring resonator," presented at the Proc. CLEO, San Jose, CA, USA, 2013, CM11.3.
- [12] C. Kopp, S. Bernabe, B. B. Bakir, J.-M. Fedeli, R. Orobtcouk, F. Schrank, H. Porte, L. Zimmermann, and T. Tekin, "Silicon photonic circuits: On-CMOS integration, fiber optical coupling, and packaging," *IEEE J. Sel. Topics Quantum Electron.*, vol. 17, no. 3, pp. 498–509, May/Jun. 2011.
- [13] K. Xu, L. G. Yang, J. Y. Sung, Y. M. Chen, Z. Z. Cheng, C. W. Chow, C. H. Yeh, and H. K. Tsang, "Compatibility of silicon Mach-Zehnder modulators for advanced modulation formats," *J. Lightwave Technol.*, vol. 31, no. 15, pp. 2550–2554, Aug. 2013.
- [14] X. Chen, C. Li, C. K. Y. Fung, S. M. G. Lo, and H. K. Tsang, "Apodized waveguide grating couplers for efficient coupling to optical fibers," *IEEE Photon. Technol. Lett.*, vol. 22, no. 15, pp. 1156–1158, Aug. 2010.